CrystEngComm

Cite this: *CrystEngComm*, 2012, **14**, 6404–6411

www.rsc.org/crystengcomm

PAPER

The structure–property relationship of four crystal forms of rifaximin†

Dario Braga,*[a] Fabrizia Grepioni,*[a] Laura Chelazzi,[a] Manuela Campana,[b] Donatella Confortini[b] and Giuseppe C. Viscomi[b]

Received 8th June 2012, Accepted 3rd August 2012
DOI: 10.1039/c2ce25920f

The crystal structures of four crystal forms of rifaximin, named α, β, δ and ε, have been elucidated by a combination of single crystal and powder diffraction experiments with synchrotron and X-ray sources. The crystal structures of the δ and ε forms have been determined from powder diffraction data alone. Hot stage microscopy has also been of paramount importance in the understanding of the β → α conversion process.

1. Introduction

In 2008, we reported the identification of five different crystal forms of the synthetic antibiotic rifaximin (4-deoxy-40-methyl-pyrido[10,20-1,2]imidazo-[5,4-c]rifamycin SV),[1] manufactured by Alfa Wassermann S.p.A. Rifaximin is a broad spectrum locally acting antibiotic against Gram-positive and Gram-negative, aerobic and anaerobic organisms.[2] Due to the lack of systemic absorption, rifaximin has only local action (*e.g.* in the gastrointestinal tract) and has an excellent safety profile. The method of production of rifaximin was reported in 1989.[3]

The existence of different crystal forms of rifaximin was ascertained and their impact on parameters such as solubility, intrinsic dissolution and bioavailability were investigated at the time of patenting and were reported for the different crystal forms.[1,4] All the crystal forms were investigated by X-ray powder diffraction.[1] In the same year, a structure of the β-form, with a water content of 8.40% w/w, was reported by Bacchi *et al.*,[5] while a bromine analogue had been reported much earlier.[6] All crystal forms of rifaximin are obtained from either crystallization (β- and γ-forms) or different drying conditions (α-, δ- and ε-forms).[4] In particular, the β-form is obtained from wet rifaximin after partial drying, while the α- and δ-forms are obtained by more extensive drying *i.e.* to a water content of between 4 and 6% (w/w) for the δ-form and less than 3% for the α-form. The ε-form can only be obtained by drying the δ-form while this last process never results in the formation of the α-form. The relationship between the rifaximin crystal forms and the preparation conditions is depicted in Scheme 1.

Clearly, such a complex phase relationship, in view of the substantially different physicochemical properties of solid rifaximin in its different forms, calls for a deeper understanding of the structure–property relationship. The degree of hydration seems to play a key role, although the path leading from one form to the other is not irrelevant: both the α- and ε-forms are characterized by a low water content but they are not directly related. Therefore, it would be very useful to know how the water molecules interact with rifaximin and/or among themselves in the crystal packing. This knowledge would then cast some light on the mechanisms of (inter)conversion and on the reason for the increased/decreased stability of each form with respect to the others.

Many molecular compounds exist as different crystal forms, such as hydrates that may contain stoichiometric or non-stoichiometric amounts of water molecules. Chemical and physical properties, such as solubility and dissolution rate, may differ between polymorphs, which may significantly affect the absorption *in vivo* as well as between the anhydrous and hydrated forms of a same API. Changes in the crystal form, whether as transitions between true polymorphs or between solvates/hydrates can occur, sometimes unexpectedly, during the manufacturing process, emphasizing the importance of knowing

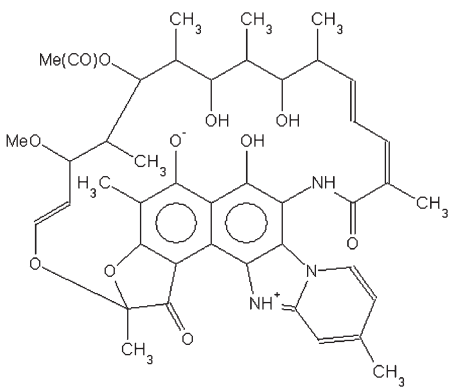

Scheme 1 Sketch of the rifaximin molecule.

[a]*Dipartimento di Chimica "G. Ciamician", Università di Bologna, via Selmi 2-40126 Bologna, Italy. E-mail: fabrizia.grepioni@unibo.it; Fax: +39 051 2099456*
[b]*Alfa Wassermann S.p.A., via Ragazzi del 99, 5, 40133 Bologna, Italy*
† Electronic supplementary information (ESI) available: CIF files for all compounds; comparisons between calculated powder patterns for all structures reported in the present work and experimental patterns from ref. 1 for patented α, β, δ and ε forms of rifaximin. CCDC reference numbers 886509–886516. For ESI and crystallographic data in CIF or other electronic format see DOI: 10.1039/c2ce25920f

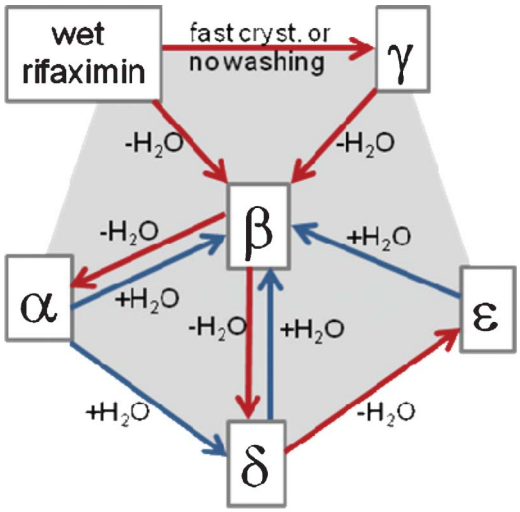

Scheme 2 The relationship between the various crystal forms of rifaximin.

and being able to control the crystal form, particularly in the case of pharmaceutical compounds. It is undisputable that the investigation of the diverse crystal forms in which a given molecule can appear has become one of the most active fields of research and a source of innovation in sectors where the production, transport, distribution marketing and exploitation of the chemicals as a solid formulation is relevant. This is particularly true for drugs but also holds well for agrichemicals, nutrichemicals, explosives, pigments *etc.*

Much of this interest and knowledge stems from the seminal work of a few pioneers, such as McCrone and Leiserowitz and to the studies and active dissemination by Joel Bernstein.[7] Under the pressure of ethical and intellectual property issues, the investigation of crystal polymorphism emerged from academic laboratories to become an industrial objective as well as an instrument for intellectual property protection and patenting.[7g]

The formation of hydrates, as of any other solvate crystal, is often unpredictable and the role of water in stabilizing the crystal packings, and hence on the bulk materials properties, such as hydration/dehydration, physico-chemical stability, wettability, comminution and tableting properties,[8a] is difficult to understand. Even more so when the same compound shows a non-stoichiometric behaviour, *i.e.* it is stable in a given crystal structure in a wide range of water content.[8b]

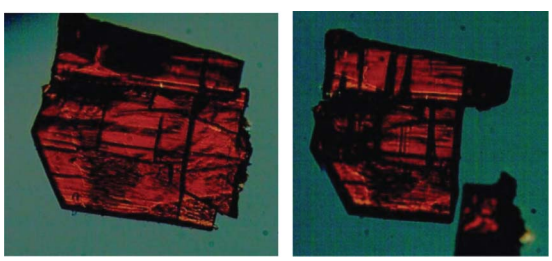

Fig. 1 The result of a typical drying process with P_2O_5: a single crystal of rifaximin form β (left) converts into a single crystal of rifaximin form α (right), which is then used for an X-ray single crystal data collection.

Several examples of hydrates have been studied in detail by Grant.[9] Theophylline forms an anhydrate and a monohydrate, which are present in mixtures of organic solvents and water depending on the water concentration: if the water activity value is less than 0.25, the anhydrate is the only species present, whereas at values greater than 0.25, the monohydrate is the most stable form.[9a] Anhydrous crystalline ampicillin has also been shown to be kinetically stable for several days in MeOH–H_2O mixtures over the whole range of water activity. Even though the crystalline trihydrate is more thermodynamically stable and less soluble than the anhydrate, interconversion occurs only with the addition of seeds and with a water activity value greater than 0.381.[9b] A useful classification scheme, proposed by Morris and Rodriguez-Hornedo,[10] considers three categories of crystalline hydrates, *i.e.* isolated site hydrates, channel hydrates and metal-ion-associated hydrates. As we will show in the following sections, rifaximin hydrates fall into both the first two categories.

With the aim of learning more about the rifaximin crystal forms, we have started a thorough investigation to determine the crystal structure of each form of rifaximin. In order to do so, we have used crystallography, single-crystal and powder diffraction. Rifaximin is not a small molecule, however, and in order to obtain sufficient information from the powder samples, we resolved to use X-ray radiation from synchrotron sources besides that available from conventional laboratory instruments.

The possibility of obtaining good quality single crystals of the β-form of rifaximin has strong implications on the characterization of the α-form, as the α-form can only be obtained *via* dehydration of the β-form. This process is normally conducted by moderate heating of a crystalline powder sample of the β-form. Dehydration of the β-form in a SCSC process (single crystal to single crystal), on the contrary, is not generally a feasible process as the cell parameters of the β- and α-forms are significantly different and therefore, the crystal experiences internal pressures during the dehydration process that easily cause crystal disintegration.[11]

Good quality crystals, such as those obtained by the procedure described here, can be dehydrated in mild conditions *i.e.* at room temperature in the presence of P_2O_5, yielding single crystals of the α-form of rifaximin, even if the crystals break (see Scheme 2). As a consequence, the collection of single crystal data *via* X-ray diffraction becomes possible and molecular and crystal structure determination of rifaximin form α can be obtained (Fig. 1).

In view of the need to gather reliable structural information, several diffraction experiments have been carried out for each crystal form of rifaximin and will be discussed in the following sections. Three crystal structures for the α-form and two new

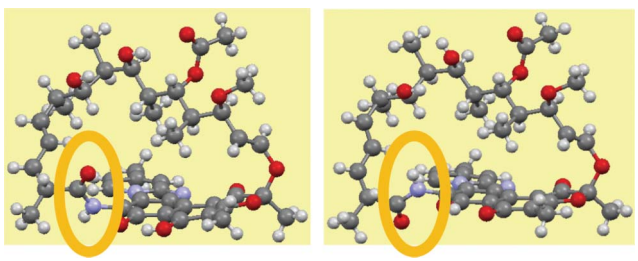

Fig. 2 Different conformations at the amidic junction in the two independent molecules of rifaximin α_0.

crystal structures for the β-form have been determined from the single crystal data, while one crystal structure for the δ-form and one for the ε-form have been determined from the powder data.

2. Results and discussion

All forms of rifaximin are non stoichiometric in that they can exist as a given crystal structure within a certain range of water content. For this reason, we have chosen to label all the structures obtained with Greek letters corresponding to the main form, as previously reported by us, with the addition of an index corresponding to the number of water molecules per formula unit, as determined from the diffraction data. Clearly, while this figure is unique in the case of the single-crystal data (see below), in the case of the δ and ε forms, whose structures have been determined from the powder data, the water content is the result of an average over the composition of the powder sample used for data collection. In the following sections, the structures will be indicated as α_0, $\alpha_{0.5}$, $\alpha_{1.5}$, β_3, $\beta_{4.5}$, δ_2 and $\varepsilon_{0.5}$.

One point however, needs to be addressed before proceeding. The water content determined from the diffraction data and from the powder diffraction experiment is the result of an average over all the crystallites constituting the sample from the crystallization batch. In the case of the single crystals, on the other hand, the average is over the total number of unit cells forming the crystal used for that specific experiment. Obviously, if every unit cell is fully occupied, this averaging "through space" leads to 100% occupancy and hence to a precise stoichiometric ratio.

The presence/absence of water molecules in specific crystalline positions can have a low-to-moderate effect on the cell axes dimensions and therefore on the position of the diffraction peaks. In addition to this, the intensity of specific peaks can vary. This may allow for a better interpretation of the X-ray powder diffractograms as shifts in the patterns can be correctly attributed to the presence of the same form but with a different water content. The structure reported by Bacchi *et al.*[5] will be denoted as β_4. A list of the structures described in the present work together with their respective water content is presented in Table 1.

All the structures of rifaximin, which is chiral, crystallize in the monoclinic $P2_1$ space group, with two independent molecules and a variable number of water molecules in the asymmetric unit. Analogously to what was observed for β_4, in all cases the two independent molecules are related by a *pseudo* two-fold axis and differ only for the local conformation at the amidic junction (see the comparison in Fig. 2). The "open conformation" of the *ansa* chain[5] is adopted in all cases.

All the rifaximin molecules analysed in the present work are shown in Fig. 3 and the pictures have a common orientation of the chromophore. It can be seen that in all cases, the open conformation of the *ansa* chain is maintained.

In all the crystals of rifaximin, the packing is based on pairs of independent molecules arranged face-to-face, as shown in Fig. 4 and 5. Whether the relevant interactions between the molecules are of the π–π stacking type or depend simply on the "shape factor", *viz.* the fact that face-to-face pairing better optimises space occupation, or on a combination of the two factors is difficult to establish. In addition to the π–π stacking, the association is assisted by an intermolecular hydrogen bond between the amidic NH group of one molecule and the CO group of the second molecule within the pair. This type of

Table 1 Rifaximin structures presented in this work, with their respective water content

Name	$n H_2O$[a]	Structure solution from	Radiation source	*T*/K	water% w/w
α_0	0	SC	synchrotron	295	—
$\alpha_{0.5}$	0.5	SC	synchrotron	100	1.1
$\alpha_{0.5}$	0.5	SC	conventional	295	1.1
$\alpha_{1.5}$	1.5	SC	conventional	295	3.3
$\beta_{3.0}$	3.0	SC	conventional	295	6.4
β_4[b]	4.0	SC	conventional	295	8.4
$\beta_{4.5}$	4.5	SC	synchrotron	295	9.4
δ_2	2.0[c]	powder	synchrotron	295	4.4
$\varepsilon_{0.5}$	0.5[c]	powder	synchrotron	295	1.1

[a] Number of water molecules in the formula unit. [b] From Ref. 5. [c] This value represents the number of water molecules averaged for the crystallites constituting the powder sample used for data collection. SC = single crystal.

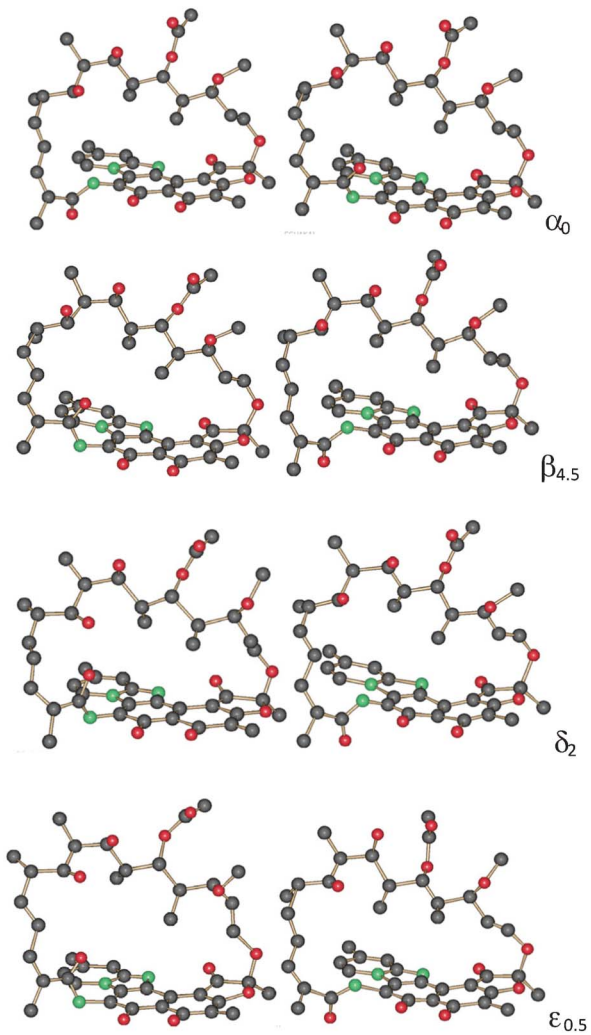

Fig. 3 Ball-and-stick representation of the two rifaximin molecules present in the asymmetric unit of α_0, $\beta_{4.5}$, δ_2 and $\varepsilon_{0.5}$ forms. It can be seen that in all cases the *ansa* chain is in an open conformation.

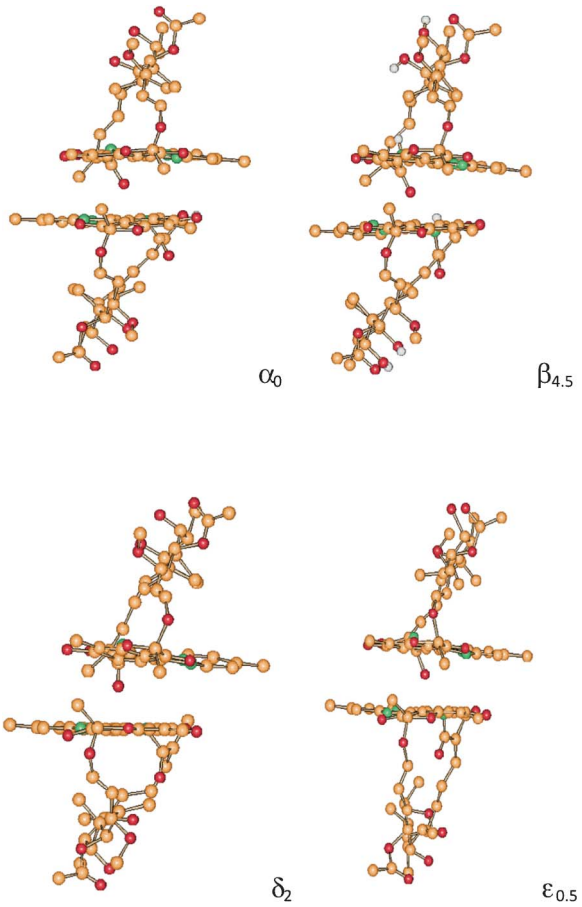

Fig. 4 Dimeric units in crystalline rifaximin, showing the progressive difference in the relative orientation of the two independent molecules in each asymmetric unit. This difference is barely detectable on passing from α_0 to $\beta_{4.5}$, while it is more pronounced in crystalline δ_2 and even more so in rifaximin $\varepsilon_{0.5}$.

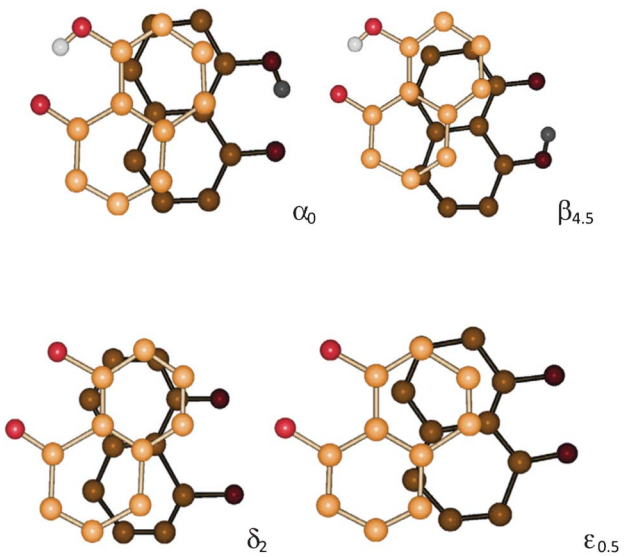

Fig. 5 Different relative orientations of the two independent molecules can be appreciated if the six-membered rings belonging to the chromophore systems are superimposed.

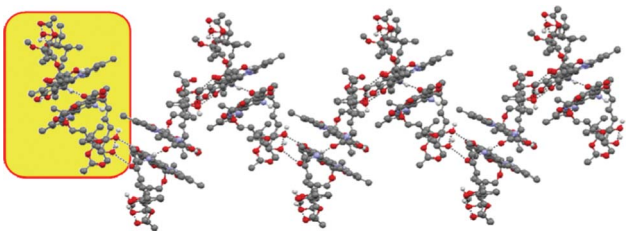

Fig. 6 Zigzag ribbon of rifaximin molecules extending along the *b*-axis direction in rifaximin α.

packing arrangement has been observed, in addition to β_4, in at least six crystals of rifamycins[5] and is responsible for the fact that the two molecules show different conformations of the amido group (as shown in Fig. 2).

Rifaximin dimers are linked together *via* hydrogen bonds involving the OH groups on the *ansa* chain, resulting in zigzag ribbons that extend along the *b*-axis (see Fig. 6). The interlocking of the rifaximin molecules on adjacent ribbons (see Fig. 7) gives rise to an infinite layer parallel to the *bc*-plane.

Alternatively, the packing in all forms of rifaximin can be seen as a juxtaposition of molecular rods extending along the *c*-axis direction (see Fig. 8). In addition to a change in the relative orientation of the rifaximin molecules within a dimeric pair, the α-, β-, δ- and ε-forms present a different relative arrangement of the molecular rods, which seem to "slide" on passing from one form to the other. The resulting orientation of the chromophore planes involved in the π-stacking interactions is evidenced by the coloured segments in Fig. 9.

Fig. 10 shows how the zigzag-pattern, which is due to the relative orientation of the dimers, is exactly the same within the α- and β-forms, irrespective of the water content: the addition of 1.5 water molecules to α_0 does not alter the rifaximin distribution and orientation in its crystal, while the addition of the same amount to $\alpha_{1.5}$ results in the phase transition to rifaximin β-form.

Rifaximin usually contains water and some forms are more prone to water absorption than others. Rifaximin α is known to take up water up to *ca.* 3% water content and then to convert

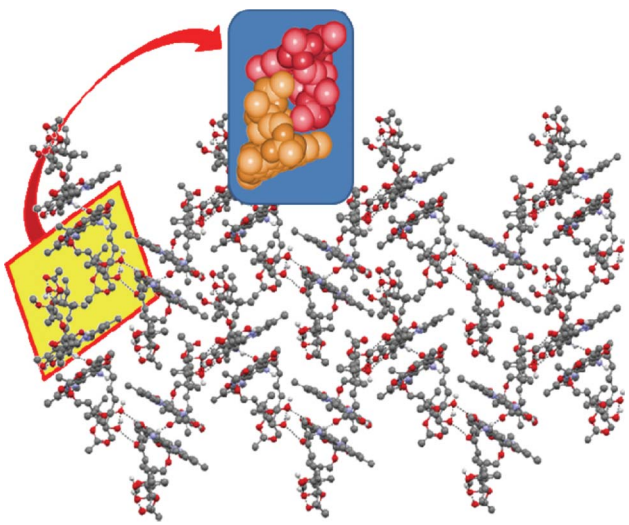

Fig. 7 Formation of a 2D molecular layer parallel to the *bc*-plane in crystalline α_0.

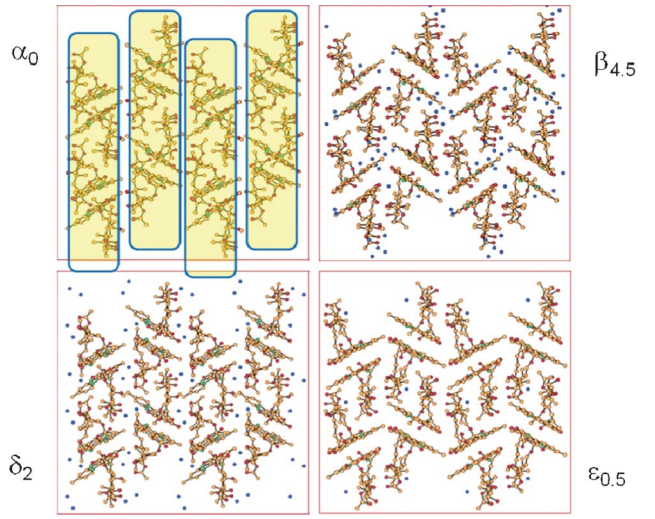

Fig. 8 Molecular rods extending along the *c*-axis in rifaximin α_0, $\beta_{4.5}$, δ_2 and $\varepsilon_{0.5}$.

into the β-form or δ-form, depending on the conditions. Obtaining the single crystal data for anhydrous rifaximin, α_0, is not an easy task as α_0 readily absorbs water from the air. The single crystal data for rifaximin α_0 could be obtained only at room temperature as at 150 K, the use of a nitrogen flow could not prevent some degree of water condensation and although synchrotron radiation was employed, thus allowing for a very fast data collection, the resulting data showed the uptake of water and formation of $\alpha_{0.5}$. Data for $\alpha_{0.5}$ was also collected at room temperature with a conventional X-ray source. An $\alpha_{1.5}$ sample was also characterized, which represents the upper limit for water in this hydrated form.

The fact that rifaximin α possesses at least one water molecule per dimeric unit can be explained if one examines the hydrogen bonding interactions involving the amido groups on the two molecules in α_0 (Fig. 11). The NH group not involved in the

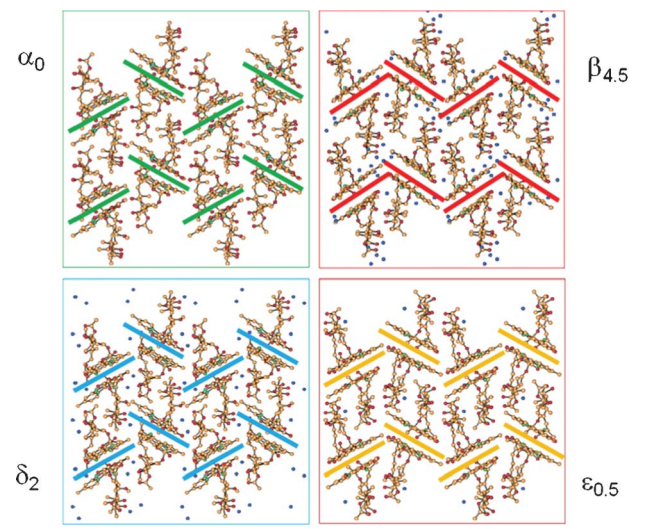

Fig. 9 The relative orientation of the chromophore planes involved in the π-stacking interactions, as evidenced by the coloured segments, in crystalline rifaximin α_0, $\beta_{4.5}$, δ_2 and $\varepsilon_{0.5}$.

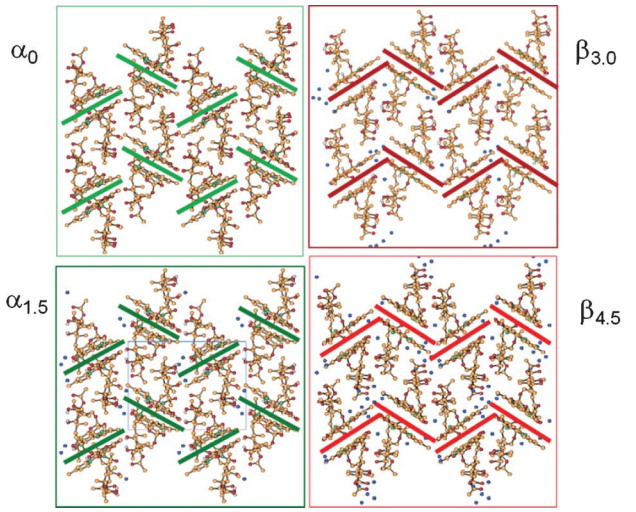

Fig. 10 The relative orientation of the dimeric units in the α- or β-forms is not altered if the water content is within the range of stability for that form.

intra-dimer hydrogen bond does not interact at close distances with hydrogen bonding acceptor groups as this is addressed by the water molecule that enters the *ansa* chain in $\alpha_{0.5}$, as can be appreciated in Fig. 11a. The position of this first water molecule is also kept in $\alpha_{1.5}$ (see Fig. 11), while the second and third water molecules interact with the OH groups belonging to the chromophore and the *ansa* chain.

In all the cases examined, although locating water is much more difficult in the δ- and ε-forms due to the fact that the water content is averaged for the polycrystalline sample and that the structures are solved from the powder data, there is a "niche" in one rifaximin molecule, where one water molecule can be accommodated in a "loose" way, as shown in Fig. 12 for rifaximin β_3. This niche is then closed by the second molecule in the dimer and by a third molecule of an adjacent rod in the crystal.

The location of the water molecule within the "niche" is constant within the α- and β-forms, as shown in Fig. 13. The remaining molecules cluster together outside this cavity. In rifaximin $\beta_{4.5}$, the 8 water molecules per dimer which form the cluster do not fully occupy their crystallographic positions but are randomly dispersed over ten different locations.

2.1. Hot-stage microscopy

Crystals of rifaximin β were placed on a Linkam LTS350 heating stage mounted directly on an Olympus polarizing optical microscope and heated in the temperature range of 25–60 °C, at the heating rate of 1 °C min^{-1}. In all the samples in which the *b*-axis was perpendicular to the hot-stage plane, a dramatic change in the crystal shape was observed due to the sudden increase in the monoclinic *β* angle from *ca.* 90° to *ca.* 110° (see Fig. 14). In a few cases, the rapid movement caused the single crystal to break.

3. Conclusions

In this paper we have reported the crystal structures of four crystal forms of rifaximin. The structural characterization has

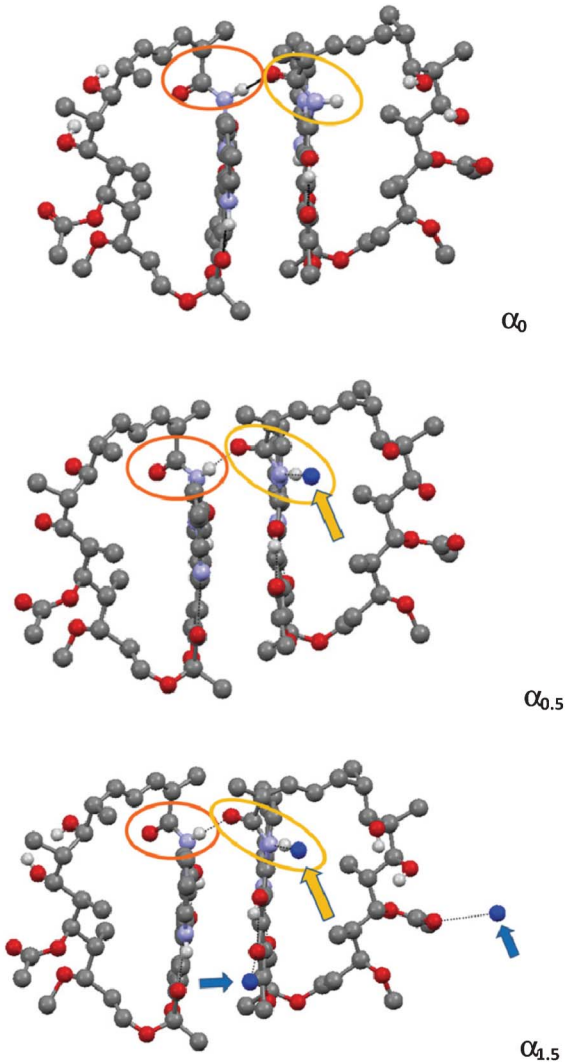

Fig. 11 The two hydrogen bonded amido groups in a rifaximin dimer: one of the two NH_{amido} groups (circled in orange) is always involved in the NH···O hydrogen bond while the second NH_{amido} is not involved in any relevant hydrogen bond interactions in rifaximin α_0. This is where the first (yellow arrow) water molecule (in blue) enters the system in rifaximin $\alpha_{0.5}$; the blue arrows indicate the location of the additional water molecules rifaximin $\alpha_{1.5}$.

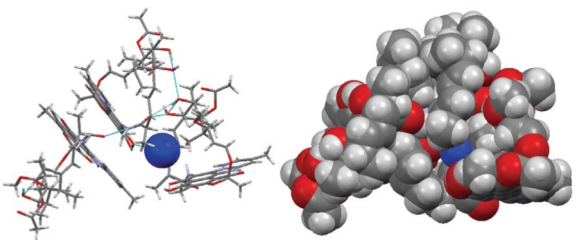

Fig. 12 The water molecule in the "niche" is in close contact with the $OH\cdots O^-$ intra-HB and it is found in all the β structures. The position is similar to the one observed in the α-form but in that case, the interaction with the NH_{amido} group is closer.

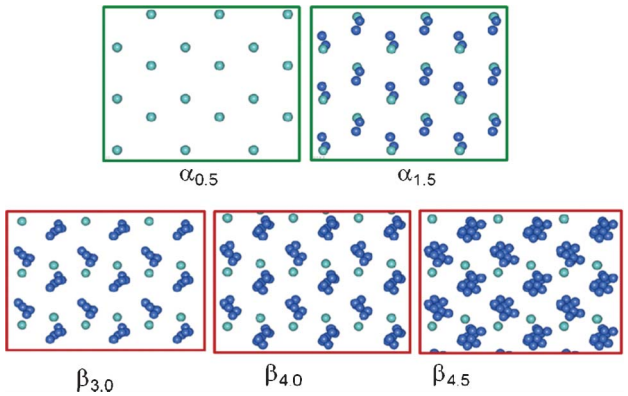

Fig. 13 Progressive clustering of water molecules on passing from $\alpha_{0.5}$ to $\beta_{4.5}$. Note how the position of the "first" water molecule (light blue) is left unchanged in all the structures (this is the water molecule linked to the NH_{amido} group in the α-form and accommodated in the niche in the β-form).

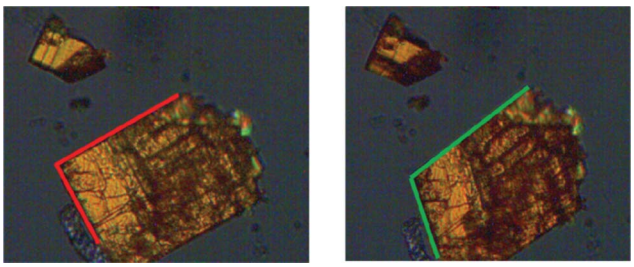

Fig. 14 Optical images of a large rifaximin single crystal: (a) β-form at 25 °C (monoclinic *β* angle, shown in red, *ca.* 91°); (b) at 50 °C the β-form → α-form transformation is complete and the monoclinic *β* angle, shown in green, is now *ca.* 110°.

been instrumental to the understanding of the phase relationship and of the hydration–dehydration processes which characterize this class of hydrates. The extent of hydration is of great importance with drugs. As observed in the case of rifaximin form β, and also for rifaximin form α, the water content can be shown to vary when single crystals are examined, passing from zero to 1.5 water molecules per rifaximin molecule, depending on the dehydration conditions and the collection technique utilized. A slight variation in the cell parameters and water molecules position/occupancy results in slight variations in the position/intensity of the peaks in the calculated diffractograms of the various α single crystals.

It is important to stress that the modifications of the diffraction patterns of the α-and β- forms due to different water content/positions are much less relevant than those observed for the β-form to α-form transformation, which is accompanied by a sudden, relevant change in the cell parameters.

Experimental details

All reagents and solvents were purchased from Sigma-Aldrich and used without further purification.

Crystallization of the rifaximin β-form

A suspension of rifaximin α in ethanol–demineralized water was heated with stirring until complete dissolution was observed. The solution was allowed to evaporate at room temperature, yielding orange single crystals of rifaximin β. Single crystals of rifaximin β were then dried with P_2O_5 in a desiccator, yielding single crystals of rifaximin α with a variable water content.

X-ray single crystal diffraction

The single-crystal data for two single crystals of the α- and β-forms of rifaximin for all compounds were collected at RT on an Oxford X′Calibur S CCD diffractometer equipped with a graphite monochromator (Mo–Kα radiation, λ = 0.71073 Å). The data collection and refinement details are listed in Table 2. To obtain data with a high resolution, single crystals of rifaximin α and β were collected on a XRD1 beamline at ELETTRA syncrothron (Trieste, Italy) with λ = 1.0 at room temperature, and at 100 K with a Cryogen system MARSCH300. The structures were solved by direct methods and refined by full-matrix least-squares on all F^2 using SHELXL97.[12a] Hydrogen atoms were partly located on the Fourier difference maps, refined isotropically and partly added in calculated positions. Anisotropic displacement parameters were refined for C and N atoms in the structures obtained in our laboratory and were refined for all non-hydrogen atoms in the structures obtained using the XRD1 beamline. The data for $\alpha_{0.5}$, $\alpha_{1.5}$ and β_3 are of poor quality, especially for the α-form of rifaximin, where single crystals are obtained *via* dehydration of the β-form. In addition to this, in the case of the X-ray data, diffraction at high angles is scarce and this is the reason for the low number of reflections collected at higher angles.

The program PLATON[12b] was used to calculate the hydrogen bonding interactions. SCHAKAL99[12c] and Mercury[12d] were used for the molecular graphics.

X-ray powder diffraction

X-ray powder diffractograms were collected on a Pananlytical X′Pert PRO automated diffractometer with Cu–Kα radiation and an X′Celerator detector equipped with an Anton Paar TTK 450 low-temperature camera. The program PowderCell[12e] was used to calculate the X-ray powder patterns on the basis of the single crystal data. The identity of the bulk material obtained and the structures obtained from single crystals were verified by comparing the calculated and observed powder diffraction patterns.

Structural determinations from powder data.

X-ray diffraction patterns of rifaximin δ and ε were recorded at the diffraction beamline at the ELETTRA synchrotron radiation facility in Trieste. The diffraction data for the powder sample encapsulated in a 0.3 mm diameter capillary was measured using X-rays with a wavelength of 1.0 Å at room temperature. The powder diffraction data was analyzed with the Highscore plus software. 30 peaks were chosen in the 2θ range of 5–40° and the unit cell parameters were found by using the DICVOL algorithm.[13] The powder data for rifaximin δ showed impurities

Table 2 Rifaximin structures presented in this work, with their respective water content

	Rifaximin α				Rifaximin β			Rifaximin δ	Rifaximin ε
	Synchrotron		X-ray		X-ray	X-ray (Ref. 5)	Synchrotron	Synchrotron	Synchrotron
Formula	$C_{43}H_{51}N_3O_{11}$	$C_{43}H_{52}N_3O_{11.5}$	$C_{43}H_{52}N_3O_{11.5}$	$C_{43}H_{54}N_3O_{12.5}$	$C_{43}H_{57}N_3O_{14}$	$C_{43}H_{59}N_3O_{15}$	$C_{43}H_{60}N_3O_{15.5}$	$C_{43}H_{55}N_3O_{13}$	$C_{43}H_{53}N_3O_{12}$
Water	0	0.5	0.5	1.5	3	4	4.5	4	1
Mr	785.88	794.89	794.89	812.90	839.93	857.93	866.95	785.88	731.83
T/K	295	100	295	295	295	295	295	295	295
λ/Å	1	1	0.71073	0.71073	0.71073	0.71073	1	1	1
Crystal system	Monoclinic	Monoclinic	Monoclinic	Monoclinic	Monoclinic	Monoclinic	Monoclinic	Monoclinic	Monoclinic
Space group	$P2_1$	$P2_1$	$P2_1$	$P2_1$	$P2_1$	$P2_1$	$P2_1$	$P2_1$	$P2_1$
a/Å	14.232(4)	14.401(4)	14.579(4)	14.492(4)	13.7960(8)	13.8420(8)	13.753(8)	13.760(7)	13.475(8)
b/Å	19.822(4)	19.662(4)	20.232(4)	20.098(4)	19.944(4)	19.863(1)	19.749(4)	20.256(1)	20.629(1)
c/Å	16.164(4)	16.153(4)	16.329(4)	16.215(4)	16.607(6)	16.721(1)	16.378(6)	16.347(3)	15.997(7)
β (°)	108.74(3)	111.04(3)	111.24(3)	111.21(3)	92.180(1)	91.709(1)	91.972(1)	106.706(1)	107.223(1)
V/Å^3	4318.2(5)	4268.6(5)	4489.3(5)	4402.7(5)	4566.1(4)	4595.3(4)	4445.8(6)	4364.0(3)	4247.4(7)
Z	4	4	4	4	4	4	4	4	4
D_c/Mg m^{-3}	1.209	1.237	1.237	1.226	1.222	—	1.295	—	—
μ/mm^{-1}	0.09	0.09	0.08	0.09	0.09	—	0.10	—	—
F(000)	1672	1692	1672	1732	1792	—	1852	—	—
2θ range/deg	$2 < 2\theta < 40$	$3 < 2\theta < 40$	$3 < 2\theta < 60$	$3 < 2\theta < 60$	$3 < 2\theta < 60$	—	$2 < 2\theta < 40$	—	—
Reflns collected	10$601	9506	20$151	15$800	19$550	—	11$822	—	—
Indip. reflns	6941	6184	6184	2415	2253	—	6019	—	—
R_{int}	5.17	2.32	17.90	16.17	16.90	—	1.30	—	—
Parameters	1027	454	992	592	503	—	1096	—	—
GoF on F^2	1.03	2.53	0.94	0.96	0.96	—	1.16	—	—
R_1(obs)	0.0805	0.1767	0.1767	0.1628	0.1948	—	0.0565	—	—
wR_2(all)	0.1063	0.1893	0.1410	0.4202	0.5247	—	0.0568	—	—
Largest ΔF max./min Å^{-3}	0.38/−0.32	1.27/−0.71	1.03/−0.31	0.67/−0.30	0.52/−0.40	—	0.78/−0.31	—	—
Rwp	—	—	—	—	—	—	—	5.00	3.04
Rp	—	—	—	—	—	—	—	2.11	2.16
R(F^2)	—	—	—	—	—	—	—	0.0345	0.0475

of the β polymorph. The structures of both δ_2 and $\varepsilon_{0.5}$ were solved by simulated annealing using all the independent ions and molecules. Simulated annealing runs with structure fragments were performed with EXPO2010, the updated version of EXPO2009.[14] All options were left as default if not specifically stated. The best solutions were chosen for Rietveld refinements.

Rietveld refinements were performed with the GSAS software.[15] Rietveld analyses were conducted starting from the solution obtained by EXPO and by treating the single molecules as rigid bodies. A shifted Chebyshev function with 16 parameters and a Pseudo-Voigt function (type 2) were used to fit the background and peak shape, respectively. A spherical harmonics model was used to describe the preferred orientation. Restraints were applied on the bond distances and angles of rifaximin. An overall thermal parameter for each atomic species of the molecules was adopted. The experimental details and structural data are listed in Table 2.

Hot-stage microscopy (HSM)

Hot Stage experiments were carried out using a Linkam TMS94 device connected to a Linkam LTS350 platinum plate. Images were collected with the imaging software Cell, from an Olympus BX41 stereomicroscope

Acknowledgements

We acknowledge financial support by the University of Bologna and MIUR. Alfa Wassermann is thanked for a research grant (LC). We thank Maurizio Polentarutti and Giorgio Bais at the Elettra facilities for the single crystal data collections on the α_0- and $\alpha_{0.5}$-forms at 150 K and the $\beta_{4.5}$-form, and for the powder data collected on δ_2 and $\varepsilon_{0.5}$. All the measurements were made possible thanks to the frame of a project between Zach System (Dr Livius Cotarca, Dr Roberto Brescello and Dr Anna Smaniotto are acknowledged) and Alfa Wassermann.

References

1 G. C. Viscomi, M. Campana, M. Barbanti, F. Grepioni, M. Polito, D. Confortini, G. Rosini, P. Righi, V. Cannata and D. Braga, *CrystEngComm*, 2008, **10**, 1074–1085.

2 (*a*) Z. D. Jiang, S. Ke, E. Palazzini, L. Riopel and H. Dupont, *Antimicrob. Agents Chemother.*, 2000, **44**, 2205–2206; (*b*) W. W. Hoover, E. Hugh Gerlach, D. J. Hoban, G. M. Eliopoulos, M. A. Pfaller and R. N. Jones, *Diagn. Microbiol. Infect. Dis.*, 1993, **16**, 111–118; (*c*) Z. D. Jiang and H. L. DuPont, *Chemotherapy*, 2005, **51**, 67–72; (*d*) C. D. Ericsson and H. L. DuPont, *Chemotherapy*, 2005, **51**, 73–80; (*e*) D. E. Baker, *Rev. Gastroenterol. Disord.*, 2005, **5**, 19–30; (*f*) A. Lamanna and A. Orsi, *Chemioterapia*, 1984, **3**, 365–367; (*g*) J. J. Descombe, D. Dubourg, M. Picard and E. Palazzini, *Int. J. Clin. Pharmacol. Res.*, 1994, **14**, 51–56.

3 V. Cannata, G. Tamagnone and S. Piani, *European Patent*, 1989, 161534, B1.

4 (*a*) G. C. Viscomi, M. Campana, D. Braga, D. Confortini, V. Cannata, P. Righi and G. Rosini, *US Patent*, 2006, No. 7,045,620; (*b*) G. C. Viscomi, M. Campana, D. Confortini, M. Barbanti and D. Braga, *PCT Patent*, 2006, WO2006/094662.

5 A. Bacchi, M. Carcelli and G. Pelizzi, *New J. Chem.*, 2008, **32**, 1725–1735.

6 M. Brufani, L. Cellai, S. Cerrini, W. Fedeli, E. Marchi, A. Segre and A. Vaciago, *J. Antibiot.*, 1984, **37**, 1623–16270.

7 (*a*) W. C. McCrone, M. M. Labes and A. Weissemberg, *Interscience*, ed. D. Fox, New York, 1965, vol. 2, p. 726; (*b*) J. Haleblian and W. McCrone, *J. Pharm. Sci.*, 1969, **58**, 911–929; (*c*) V. Benghiat and L. Leiserowitz, *J. Chem. Soc., Perkin Trans. 2*, **1972**, 1763–1768; (*d*) J. Bernstein, R. J. Davey and J.-O. Henck, *Angew. Chem., Int. Ed.*, 1999, **38**, 3440–3461; (*e*) J. Bernstein, *Polymorphism in Molecular Crystals*, Clarendon Press, Oxford, 2002; (*f*) J. Bernstein, *Cryst. Growth Des.*, 2011, **11**, 632–650; (*g*) A. Bulow, *Innovation Policy and the Economy 4*, ed. A. B. Jaffe, J. Lerner and S. Stern, The MIT Press, Cambridge, 2004, pp. 145-185.

8 (*a*) K. R. Morris, U. J. Griesser, C. J. Eckhardt and J. G. Stowell, *Adv. Drug Delivery Rev.*, 2001, **48**, 91–114; (*b*) H. G. Brittain, K. R. Morris and S. X. M. Boerrigter in *Structural aspects of solvatomorphic systems, in Polymorphism in Pharmaceutical Solids*, ed. H. G. Brittain, 2nd Edition, Informa Healthcare USA, Inc., New York, 2009, p. 249.

9 (*a*) H. Zhu, C. Yuen and D.J.W. Grant, *Int. J. Pharm.*, 1996, **139**, 135–151; (*b*) H. Zhu and D. J. W. Grant, *Int. J. Pharm.*, 1996, **139**, 33.

10 K. R. Morris and N. Rodríguez-Hornedo in *Encyclopedia of Pharmaceutical Technology*, ed. J. Swarbrick and J, Boylan, volume 7, pages 393–440, Marcel Dekker, New York, 1993.

11 I. Halasz, *Cryst. Growth Des.*, 2010, **10**, 2817–2823.

12 (*a*) G. M. Scheldrick, SHELXL97: Program for Crystal Structure Determination, University of Göttingen, Germany, 1997; (*b*) A. L. Speck, *PLATON: Acta Crystallogr., Sect. A*, 1990, **46**, C34; (*c*) E. KellerSCHAKAL99: Graphical Representation of Molecular Models; University of Freiburg, Freiburg, Germany, 1999; (*d*) MERCURY 3.0: New Features for the Visualization and Investigation of Crystal Structures; C. F. Macrae, I. J. Bruno, J. A. Chisholm, P. R. Edgington, P. McCabe, E. Pidcock, L. Rodriguez-Monge, R. Taylor, J. van de Streek and P. A. Wood, *J. Appl. Cryst.*, 2008, **41**, 466-470; (*e*) PowderCell programmed by W. Kraus and G. Nolze (BAM Berlin)©, subgroups derived by Ulrich Müller (Gh Kassel).

13 A. Boultif and D. Louer, *J. Appl. Crystallogr.*, 2004, **37**, 724–731.

14 A. Altomare, M. Camalli, C. Cuocci, C. Giacovazzo, A. Moliterni and R. Rizzi, *J. Appl. Crystallogr.*, 2009, **42**, 1197–1202.

15 A. C. Larson and R. B. Von Dreele, *General Structure Analysis System (GSAS)*, Los Alamos National Laboratory Report LAUR, 86-748, 2000.